$CD103^+CD11b^+$ mucosal classical dendritic cells initiate long-term switched antibody responses to flagellin

Flores-Langarica, A; Müller Luda, K; Persson, E K; Cook, C N; Bobat, S; Marshall, J L; Dahlgren, M W; Hägerbrand, K; Toellner, K M; Goodall, M D; Withers, David; Henderson, I R; Johansson Lindbom, B; Cunningham, Adam; Agace, W W

DOI:
10.1038/mi.2017.105

OPEN

CD103$^+$CD11b$^+$ mucosal classical dendritic cells initiate long-term switched antibody responses to flagellin

A Flores-Langarica[1], K Müller Luda[2], EK Persson[2], CN Cook[1], S Bobat[1], JL Marshall[1], MW Dahlgren[2], K Hägerbrand[2], KM Toellner[1], MD Goodall[1], DR Withers[1], IR Henderson[3], B Johansson Lindbom[2,4], AF Cunningham[1,3,5] and WW Agace[2,4,5]

Antibody responses induced at mucosal and nonmucosal sites demonstrate a significant level of autonomy. Here, we demonstrate a key role for mucosal interferon regulatory factor-4 (IRF4)-dependent CD103$^+$CD11b$^+$ (DP), classical dendritic cells (cDCs) in the induction of T-dependent immunoglobulin G (IgG) and immunoglobulin A (IgA) responses in the mesenteric lymph node (MLN) following systemic immunization with soluble flagellin (sFliC). In contrast, IRF8-dependent CD103$^+$CD11b$^-$ (SP) are not required for these responses. The lack of this response correlated with a complete absence of sFliC-specific plasma cells in the MLN, small intestinal lamina propria, and surprisingly also the bone marrow (BM). Many sFliC-specific plasma cells accumulating in the BM of immunized wild-type mice expressed $\alpha_4\beta_7^+$, suggesting a mucosal origin. Collectively, these results suggest that mucosal DP cDC contribute to the generation of the sFliC-specific plasma cell pool in the BM and thus serve as a bridge linking the mucosal and systemic immune system.

INTRODUCTION

Flagellin is the filament protein component of bacterial flagella. Extracellular flagellin is recognized primarily through Toll-like receptor 5 (TLR5) and this can induce profound responses in innate and adaptive immune cells.[1] Immunization with purified, soluble flagellin (sFliC) protein from *Salmonella* Typhimurium is sufficient to drive T- and B-cell responses against itself and co-immunized antigens in the absence of additional adjuvant.[2–5] This autoadjuvant activity of flagellin has led to its use as a carrier protein in a number of vaccine strategies,[6–8] including an influenza fusion vaccine tested in humans.[9,10] Additionally, immunization of sFliC in mice has been shown to enhance protection against viral infections[11] and radiation exposure,[12] promote antigen presentation through major histocompatibility complex class-II (MHC-II),[13] and reduce T helper cell type 1 (Th1) differentiation after coimmunization with *Salmonella* Typhimurium.[14] Although such findings indicate that flagellin is an important modulator of the adaptive immune system, the cellular mechanism(s) underlying its mode of action remain unclear.

Previously, it has been shown that systemic immunization with sFliC, given subcutaneously in the footpad or intraperitoneally, induces immunoglobulin G (IgG) responses in the spleen and concurrent IgG and IgA responses in the intestinal draining mesenteric lymph nodes (MLNs).[15] This unexpected induction of intestinal responses after systemic immunization was TLR5 dependent and associated with the rapid and extensive recruitment of antigen-loaded CD103$^+$ classical dendritic cells (cDCs) into the MLN. This coincided with a decrease in the frequency of these cells in the small intestine lamina propria (SI-LP) and suggests that the autoadjuvant activity of sFliC may, in part, be mediated through the activation of mucosal CD103$^+$ cDCs.

[1]Institute of Immunology and Immunotherapy, College of Medical and Dental Sciences, University of Birmingham, Birmingham, UK. [2]Immunology Section, Lund University, Lund, Sweden. [3]Institute of Microbiology and Infection, College of Medical and Dental Sciences, University of Birmingham, Birmingham, UK and [4]Division of Immunology and Vaccinology, National Veterinary Institute, Technical University of Denmark (DTU), Kongens Lyngby, Denmark. Correspondence: A Flores-Langarica (a.floreslangarica@bham.ac.uk); AF Cunningham (a.f.cunningham@bham.ac.uk)
[5]AF Cunningham and WW Agace are joint senior authors.

Received 21 July 2017; accepted 23 October 2017; advance online publication, 20 December 2017; doi:10.1038/mi.2017.105

The intestinal mucosa contains three major subsets of cDCs: $CD103^+CD11b^+$, $CD103^+CD11b^-$, and $CD103^-$ cDCs,[16,17] that require different transcription factors for their development and survival. Deletion of the transcription factors interferon regulatory factor-8 (IRF8), BATF3, or ID2 results in a loss of intestinal and MLN $CD103^+CD11b^-$ cDCs,[18–20] whereas deletion of IRF4 and NOTCH-2 results in a loss of intestinal-derived $CD103^+CD11b^+$ cDCs in the MLN.[21,22] We, and others, have recently demonstrated that these subsets play key non-redundant roles in regulating intestinal immune homeostasis. For example, IRF4-dependent cDCs play an important role in intestinal Th17 (refs. [21,23]) and Th2 responses[24] and for driving postoperative ileitis.[25] In contrast, IRF8-dependent $CD103^+CD11b^-$ cDCs are required for the maintenance of T cells within the small intestinal epithelium and for the generation and maintenance of intestinal interferon-γ – producing Th1 cells.[26,27]

In this study, we assessed the role of mucosal cDCs in the generation of sFliC-specific IgG and IgA responses in the MLN following systemic immunization, and the impact of this response on the accumulation of plasma cells in the bone marrow (BM). We demonstrate that mucosal $CD103^+CD11b^+$ but not $CD103^+CD11b^-$ cDCs are essential for the generation of sFliC-specific responses in the MLN, and that the absence of this response affects long-term systemic antibody (Ab) response in the BM. Collectively, these results suggest that mucosal $CD103^+CD11b^+$ cDCs act as a bridge to link adaptive immune responses of the intestinal mucosa to serological memory and systemic protection.

RESULTS

DP cDCs recruited to the MLN after direct stimulation by sFliC are functional

Intraperitoneal (IP) or subcutaneous immunization with sFliC drives a TLR5-dependent accumulation of $CD103^+$ cDCs in intestinal draining MLN.[15] To determine which $CD103^+$ cDC subset accumulates in the MLN in response to sFliC, wild-type (WT) mice were immunized IP with sFliC and numbers of $CD103^+CD11b^+$ (DP), $CD103^+CD11b^-$ (SP), and $CD103^-$ cDCs in the MLN and SI-LP were assessed 24 h later by flow cytometry (for gating strategy see **Supplementary Figure S1a** online). sFliC immunized mice had an increased frequency of $CD11c^+MHC\text{-}II^{hi}$ cDCs in MLN (**Figure 1a**). In the steady state this population has been suggested to contain cDCs that have migrated from the SI-LP[28] and potentially some resident $CD8\alpha^+$ and $CD11b^+$ cDCs that have upregulated MHC-II upon activation. Within the $CD11c^+MHC\text{-}II^{hi}$ population, DP but not SP or $CD103^-$ cDC numbers increased in the MLN in response to sFliC (**Figure 1a**) that paralleled a selective loss of DP cDCs in the SI-LP (**Figure 1b**). Despite the selective increase in DP cDC numbers in MLN, sFliC immunization induced upregulation of CD40 and CD86 in all MLN cDC subsets (**Figure 1c**).

sFliC immunization failed to induce DP cDC accumulation in the MLN of mice lacking MyD88 in $CD11c^+$ cells (*Cd11c-cre.MyD88$^{fl/fl}$* mice[28]) (**Figure 1d**), indicating that sFliC may directly drive DP cDC recruitment to MLN. To assess this possibility, mixed BM chimeras were generated with BM from *Cd11c-cre.Irf4$^{fl/fl}$*mice, which lack DP cDC in MLN,[21] and *Cd11c-cre.MyD88$^{fl/fl}$* mice (**Figure 1e**). In these chimeras, DP cDCs in the MLN are MyD88 deficient, whereas other $CD11c^+$ cells are a mixture of MyD88-sufficient and -deficient cells. sFliC also failed to induce DP cDC accumulation in the MLN of these mice (**Figure 1e**). Deletion of IRF4 in *Cd11c-cre.MyD88$^{fl/fl}$* leads to the expression of green fluorescent protein (GFP)[21] in $CD11c^+$ cells and thus can be used to discriminate between $CD11c^+$ cells derived from different donor mice. Assessment of GFP expression in cDCs from the SI-LP of the chimeras showed that both *MyD88$^{fl/fl}$* (GFP^-) and *Cd11c-cre.MyD88$^{fl/fl}$* cDCs (GFP^-) were found in similar proportions in comparison with cDCs derived from *Cd11c-cre.Irf4$^{fl/fl}$* (GFP^+) donor BM (**Supplementary Figure S1b**). Collectively, these results demonstrate that sFliC signaling in DP cDCs is required for their accumulation in the MLN.

It has previously been shown that $CD103^+$ cDCs are responsible for T-cell priming in the MLN following IP immunization with sFliC.[15] To determine which of the two MLN $CD103^+$ cDC subsets underlie this response, SP and DP cDCs were fluorescence-activated cell sorted (FACS) from the MLN 24 h after IP immunization with sFliC and co-cultured with SM1 transgenic T cells that are specific for an epitope in *Salmonella* Typhimurium FliC (amino acids 427–441).[29,30] DP cDCs were far more efficient than SP cDCs at inducing SM1 T-cell division and activation as assessed by carboxyfluorescein succinimidyl ester dilution, downregulation of CD62L, and total cell counts (**Figure 1f**). Importantly, *ex vivo* addition of sFliC to the SP and DP cDC-T cell co-cultures resulted in similar SM1 T-cell division (**Figure 1f**), demonstrating that the diminished capacity of SP cDCs to present sFliC *in vivo* was not due to an inability of these cells to present antigen. Thus, DP cDCs represent the major sFliC peptide-presenting cells in the MLN.

$CD103^+CD11b^+$ DP cDCs are required for the generation of mucosal anti-sFliC IgA and IgG responses

To assess the role of MLN $CD103^+$ cDC subsets in sFliC-specific Ab responses, we used a prime–boost system as previously described.[15] First, we determined whether priming with sFliC could interfere with the accumulation of DP cDCs (for example, through the induction of antibodies) after secondary immunization. Secondary immunization induced a similar and selective accumulation of DP cDCs in the MLN as observed after primary immunization (**Figure 2a**), despite the presence of sFliC-specific IgG in the serum (**Figure 2b**).

To address the role of DP cDCs in the sFliC-specific Ab response, *Cd11c-cre.Irf4$^{fl/fl}$*mice were immunized twice with sFliC and the response was examined 4 days after boost. In marked contrast to control *Irf4$^{fl/fl}$*mice, the number of plasma cells did not increase in the MLN of *Cd11c-cre.Irf4$^{fl/fl}$*mice following boosting with sFliC (**Figure 3a**; detailed gating strategy is shown in **Supplementary Figure S1c**), suggesting a reduced sFliC-specific Ab response at this site. Consistent with

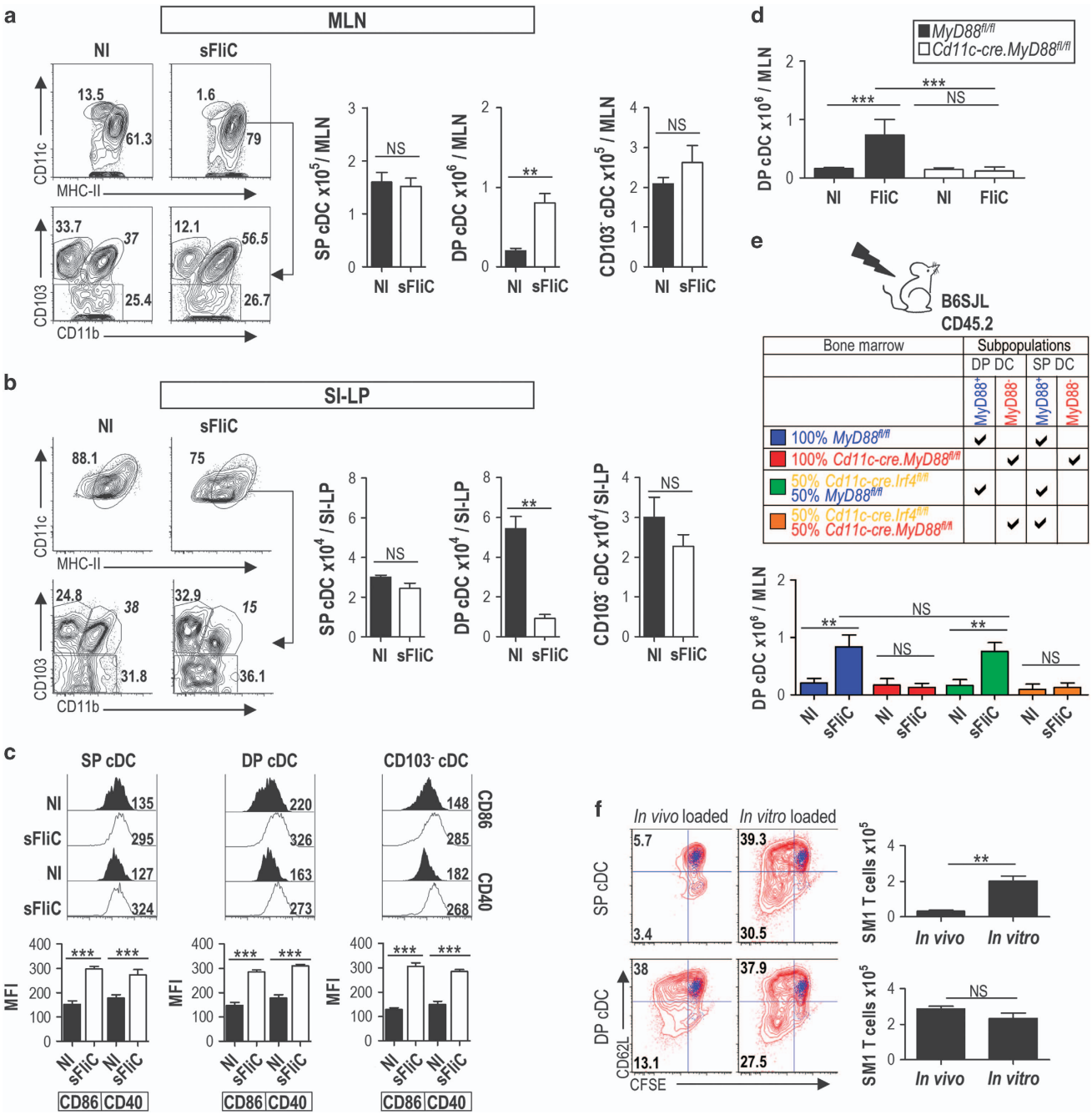

Figure 1 Soluble flagellin (sFliC) stimulates CD103$^+$CD11b$^+$ (DP) classical dendritic cells (cDCs) directly to induce their accumulation in the mesenteric lymph node (MLN) and loss from the small intestine lamina propria (SI-LP). Wild-type (WT) mice were immunized intraperitoneally (IP) with sFliC and cDC (MHC-II$^+$CD11c^{hi}) subsets evaluated in (**a**) MLN and (**b**) SI-LP 24 h later by flow cytometry. NI, nonimmunized. Representative plots with percentages for CD103$^+$CD11b$^-$ (SP), CD103$^+$CD11b$^+$ (DP), and CD103$^-$ cDC subsets are shown. Graphs show absolute numbers of the gates. (**c**) Representative histograms of expression of CD86 and CD40 on SP, DP, and CD103$^-$ cDC subsets 24 h after sFliC immunization. Graphs show mean fluorescent index (MFI). Data are mean + s.d. of 4 mice and are representative of 3 independent experiments. ***$P<0.0001$, by Mann–Whitney test, NS, not significant. (**d**) Absolute numbers of DP cDCs in the MLN of *Cd11c-cre.MyD88$^{fl/fl}$*(white) or *MyD88$^{fl/fl}$* (black) mice 24 h after sFliC immunization. Mean + s.d. ($n=6$ mice/group) of 2 independent experiments. ***$P<0.0001$, by two-way analysis of variance (ANOVA). (**e**) Lethally irradiated WT mice were reconstituted with *MyD88$^{fl/fl}$* or *Cd11c-cre.MyD88$^{fl/fl}$* bone marrow (BM) or with a 50:50 mixture of *MyD88$^{fl/fl}$* or *Cd11c-cre.MyD88$^{fl/fl}$* with *Cd11c-cre.Irf4$^{fl/fl}$* BM. Absolute numbers of DP cDCs in the MLN 24 h after immunization. Mean + s.d. ($n=8$ mice/group) from 2 independent experiments. ***$P<0.0001$, by two-way ANOVA. (**f**) MLN SP and DP cDC subsets were fluorescence-activated cell sorted (FACS) from WT mice 24 h after sFliC immunization and cultured for 4 days with carboxyfluorescein succinimidyl ester (CFSE)-labeled FliC-specific transgenic (SM1) T cells in a 1:30 ratio. sFliC (2 mg) was added to some cultures (*in vitro* loaded) as indicated. T-cell division was assessed by CFSE dilution and CD62L downregulation, blue overlay represents T cells cultured alone, and representative plots are shown. Graphs depict absolute numbers of T cells. Data are mean + s.d. ($n=4$ mice/group) from two pooled experiments. **$P<0.001$, by Mann–Whitney test.

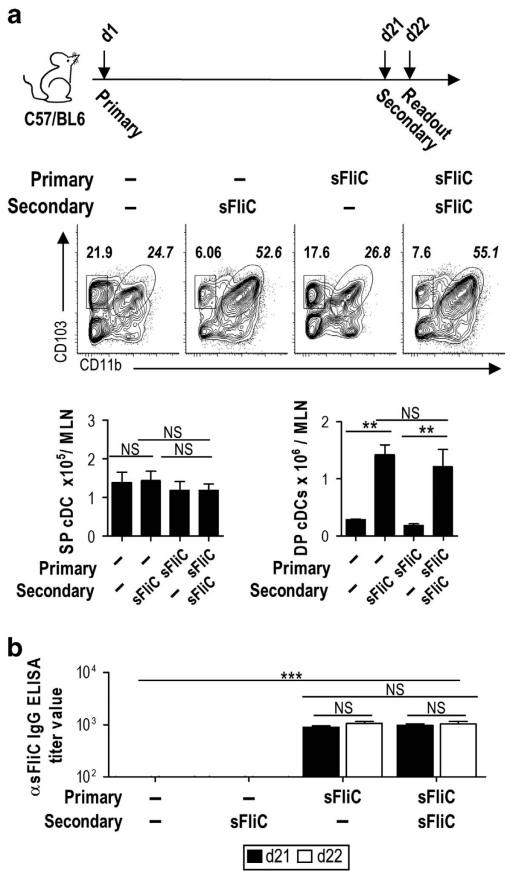

Figure 2 Secondary soluble flagellin (sFliC) immunization does not affect the mesenteric lymph node (MLN) classical dendritic cell (cDC) accumulation. (**a**) $CD103^+CD11b^+$ (DP) and $CD103^+CD11b^-$ (SP) cDC accumulation in the MLN of wild-type (WT) mice 24 h after sFliC primary or boost immunization. Representative plots with percentages for SP and DP cDC subsets. Graphs show absolute numbers of the gates. (**b**) Serum levels of anti-sFliC 21 days after SFliC immunization (black) or 1 day after boost (d22) (white) as indicated. Data are mean + s.d. ($n = 4$ mice/group) of two independent experiments. $^{**}P < 0.001$ and $^{***}P < 0.0001$, by one-way analysis of variance (ANOVA), NS, not significant.

this, sFliC-specific IgG and IgA Ab-secreting cells (ASCs) were readily detected in the MLN of *Irf4*$^{fl/fl}$but not *Cd11c-cre.Irf4*$^{fl/fl}$ mice as assessed by ELISPOT (Enzyme-Linked ImmunoSpot) (**Figure 3b**). Plasma cells derived from the MLN can migrate to the SI-LP contributing to the specific response in this site. To examine whether this element of the response was also affected, cells were isolated from the SI-LP and sFliC-specific ASCs assessed as above. As with the MLN, sFliC-specific IgG^+ and IgA^+ ASCs were detected in the SI-LP of *Irf4*$^{fl/fl}$ but not *Cd11c-cre.Irf4*$^{fl/fl}$mice (**Figure 3b**, lower panels). To exclude the possibility that the reduced numbers of sFliC-specific ASCs observed in *Cd11c-cre.Irf4*$^{fl/fl}$mice was a result of an intrinsic defect in B-cell function,[31] mixed BM chimeras were generated using a 50:50 mix of BM cells from *Irf4*$^{fl/fl}$ or *Cd11c-cre.Irf4*$^{fl/fl}$ mice with BM cells from *Rag-1*$^{-/-}$ mice. In these chimeras Irf4-dependent cDCs derive from *Rag-1*$^{-/-}$ BM, whereas the B-cell compartment derives from *Cd11c-cre.Irf4*$^{fl/fl}$ BM. RAG-$1^{-/-}$ BMs fully rescued the defect in plasma cell numbers observed in single *Cd11c-cre.Irf4*$^{fl/fl}$ chimeras (**Figure 3c** lower graph) as well as sFliC-specific IgG- and IgA-producing ASCs (**Figure 3c**), confirming that the absence of Ab response in the *Cd11c-cre.Irf4*$^{fl/fl}$mice was not due to an intrinsic B-cell defect.

In marked contrast to *Cd11c-cre.Irf4*$^{fl/fl}$mice, *Cd11c-cre.Irf8*$^{fl/fl}$ mice, which lack migratory SP cDCs and LN-resident $CD8\alpha^+$ cDCs in the MLN,[26] induced equivalent numbers of plasma cells and anti-sFliC IgG and IgA ASCs in the MLN as control *Irf8*$^{fl/fl}$mice, following sFliC prime–boost (**Figure 3d,e**). Collectively, these results demonstrate that the generation of sFliC-specific Ab responses in the MLN requires DP cDCs.

Tfh cells and germinal centre responses to sFliC in the MLN are absent in *Cd11c-cre.Irf4*$^{fl/fl}$ mice

As the Ab response to sFliC is T dependent,[3,5] we next assessed whether the absence of a sFliC-specific Ab response in the MLN of *Cd11c-cre.Irf4*$^{fl/fl}$mice reflected alterations in the generation of sFliC-specific germinal centre (GC) and T follicular helper (Tfh) cells. sFliC-specific GCs were readily detected in the MLN of *Irf4*$^{fl/fl}$ but not *Cd11c-cre.Irf4*$^{fl/fl}$ mice (**Figure 4a**) and confocal microscopy showed the presence of PD1- and BCL6-expressing Tfh-like T cells in these GCs (**Figure 4a**, lower panels). Quantification of the GC and the total sFliC-specific area per section showed that immunized *Irf4*$^{fl/fl}$ mice had significantly more area containing GC than immunized *Cd11c-cre.Irf4*$^{fl/fl}$mice (**Figure 4b**). Consistent with this finding, GC B-cell numbers increased in sFliC-immunized *Irf4*$^{fl/fl}$ but not *Cd11c-cre.Irf4*$^{fl/fl}$mice, as determined by flow cytometry (**Figure 4c**; for gating strategy see **Supplementary Figure S1c**). Similarly, the total number of Tfh cells (defined as $CD3^+CD4^+CD62L^{lo}PD1^+CXCR5^+$, for gating strategy see **Supplementary Figure S1d**) increased in the MLN of *Irf4*$^{fl/fl}$ mice but not in *Cd11c-cre.Irf4*$^{fl/fl}$mice (**Figure 4d**). In contrast, *Cd11c-cre.Irf8*$^{fl/fl}$mice displayed a similar increase in total GC area, sFliC-specific GC area, GC B cells, and Tfh cells in the MLN to *Irf8*$^{fl/fl}$ mice (**Figure 4e–h**). Thus, the defective mucosal Ab response observed in the absence of DP cDC is associated with a loss in the generation of Tfh cells and sFliC-specific GCs in the MLN.

sFliC-specific splenic ASCs are reduced in *Cd11c-cre.Irf4*$^{fl/fl}$ mice

As sFliC induces concurrent Ab responses in the spleen and MLN[15] we next determined whether *Cd11c-cre.Irf4*$^{fl/fl}$mice displayed a defective ASC response in the spleen.

First, we evaluated the cDC response in the spleen after immunization with sFliC. In contrast to the MLN, immunization with sFliC did not affect the frequency or total number of $CD4^+$ or $CD8\alpha^+$ cDCs (**Figure 5a**), although it led to increased expression of CD86 and CD40 by both subsets (**Figure 5b**). As expected,[21] splenic $CD4^+$ cDC numbers were reduced in *Cd11c-cre.Irf4*$^{fl/fl}$compared with *Irf4*$^{fl/fl}$mice in steady state (**Figure 5a**), and this difference was maintained after sFliC immunization.

When assessing the Ab response 4 days after secondary immunization, *Cd11c-cre.Irf4*$^{fl/fl}$ mice displayed a reduction in sFliC-specific IgG^+ ASCs and virtually no IgA^+ ASCs when compared with *Irf4*$^{fl/fl}$ mice (**Figure 5c**). sFliC-specific GCs

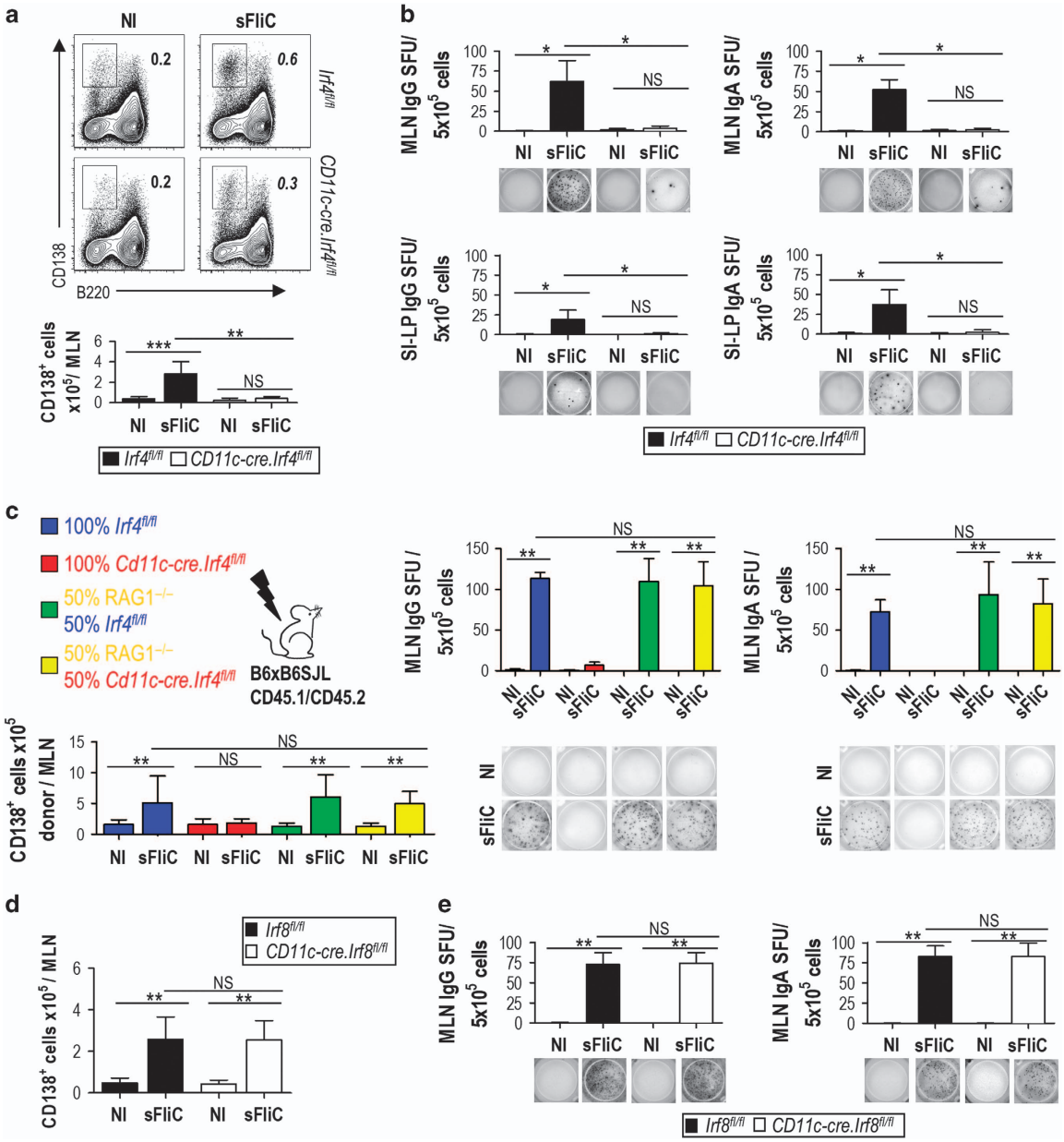

Figure 3 CD103$^+$CD11b$^+$ (DP) classical dendritic cells (cDCs) control the induction of the mucosal antibody (Ab) response to soluble flagellin (sFliC). *Irf4*$^{fl/fl}$(black) or *Cd11c-cre.Irf4*$^{fl/fl}$ (white) mice were either nonimmunized (NI) or primed and boosted with sFliC. The Ab response was evaluated 4 days after boost. (**a**) Representative plots and absolute number (graphs) of plasma cells (TCRb$^-$CD19$^+$B220^{low}CD138$^+$) in the mesenteric lymph node (MLN). (**b**) ELISPOT (Enzyme-Linked ImmunoSpot) analysis of sFliC immunoglobulin G (IgG) and immunoglobulin A (IgA) responses in the MLN and small intestine lamina propria (SI-LP). Number of spot-forming units (SFUs) per 5×10^5 cells (graphs) and representative pictures of wells (lower panels). Data are mean + s.d. ($n = 4$ mice/group) and are from one representative experiment of three performed. ***$P < 0.0001$, by two-way analysis of variance (ANOVA), NS, not significant. (**c**) Indicated bone marrow (BM) chimeras were either NI or sFliC primed–boosted. Total number of CD45.2$^+$ plasma (CD138$^+$) cells (lower left graph), sFliC-specific antibody-secreting cells (ASCs, right upper graphs) and representative ELISPOT wells (lower right) from the MLN of chimeric mice 4 days after boost. Data are mean + s.d. ($n = 4$ mice/group). ***$P < 0.0001$, by one-way ANOVA. (**d**,**e**) *Cd11c-cre.Irf8*$^{fl/fl}$ (white) or *Irf8*$^{fl/fl}$control mice (black) were either NI or sFliC primed–boosted, and the absolute number of (**d**) plasma cells and (**e**) sFLiC-specific IgG and IgA ASCs in the MLN assessed 4 days after boost. Data are mean + s.d. ($n = 8$ mice/group) from two pooled experiments. ***$P < 0.0001$, by two-way ANOVA.

were observed in the spleens of *Cd11c-cre.Irf4*$^{fl/fl}$ mice after immunization, although to a lesser extent when compared with *Irf4*$^{fl/fl}$mice (**Figure 5d**). Strikingly, splenic GC B-cell and Tfh-cell numbers were not significantly different in *Irf4*$^{fl/fl}$and *Cd11c-cre.Irf4*$^{fl/fl}$mice after sFliC immunization (**Figure 5e,f**). Thus, in contrast to the MLN, IRF4-dependent cDCs are not required for Tfh cell generation and GC induction in the spleen in response to sFliC immunization.

We hypothesized that Tfh cells were still detectable in the spleens of *Cd11c-cre.Irf4*$^{fl/fl}$ mice because CD8α^+CD11b$^-$ splenic

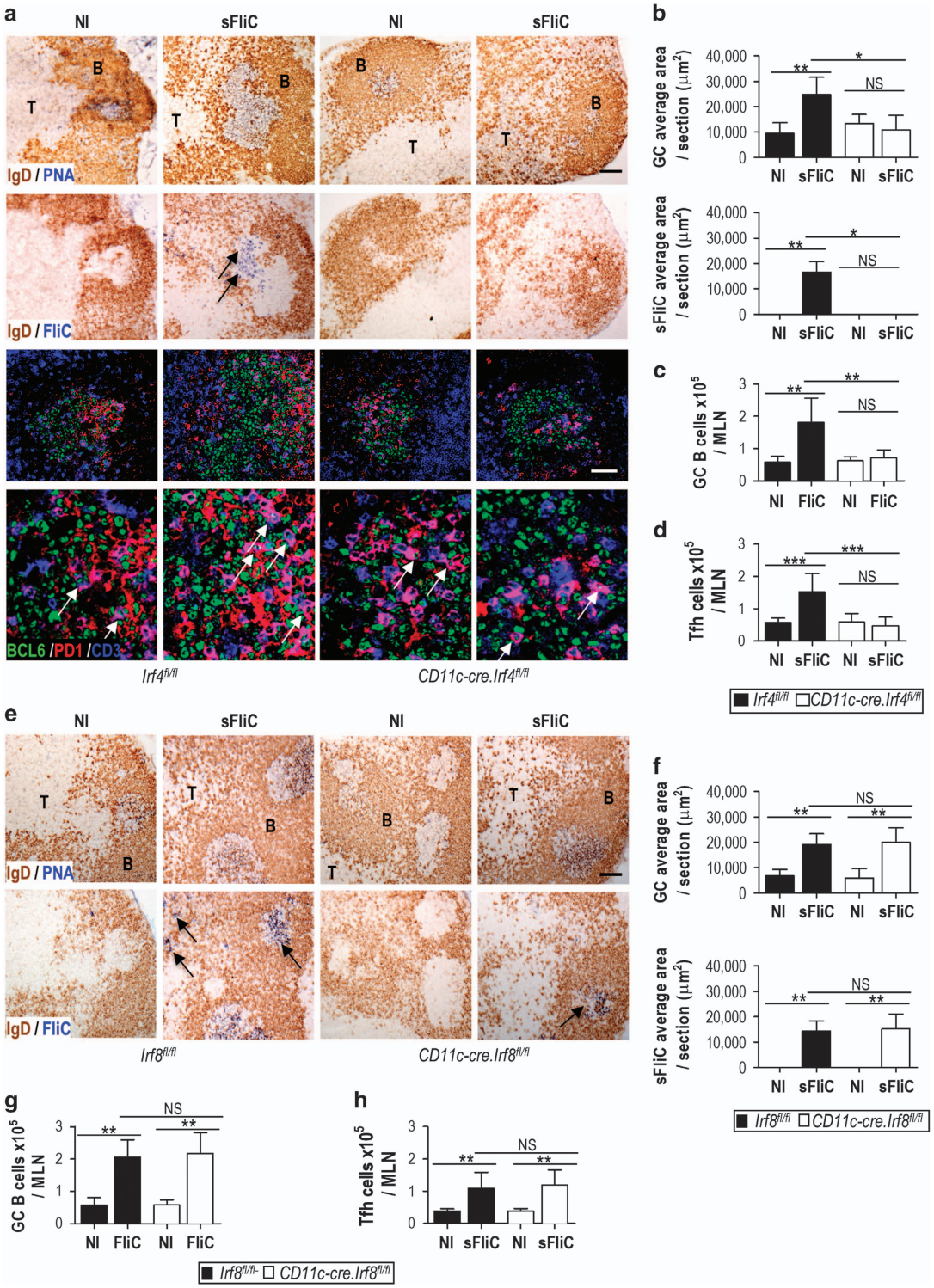

Figure 4 Soluble flagellin (sFliC)-specific germinal centre (GC) and T follicular helper (Tfh) cell induction in the mesenteric lymph node (MLN) are dependent on $CD103^+CD11b^+$ (DP) mucosal classical dendritic cells (cDCs). (**a**) Representative photomicrographs of sFliC-specific GC in the MLN of *Irf4*$^{fl/fl}$(black) or *Cd11c-cre.Irf4*$^{fl/fl}$ (white) nonimmunized (NI) or sFliC prime–boosted mice. Scale bar = 200 µm. First row, GC identification (Peanut agglutinin (PNA), blue; immunoglobulin D (IgD), brown). Second row, sFliC-specific GC (sFliC, blue; IgD, brown indicated with black arrows. T indicates T zone, B indicates B zone). Lower panel, confocal analysis of the previously selected GC stained to identify Tfh cells (BCL6, green; PD1, red and CD3, blue, indicated with white arrows). Scale bar = 50 µm. (**b**) Quantification of total GC and sFliC-specific area per section. Mean + s.d. (n = 10 sections/group, from 2 experiments *$P<0.01$, **$P<0.001$). Number of (**c**) GC B cells ($TCR^-CD138^-GL7^+CD95^+$) and (**d**) Tfh cells ($CXCR5^+PD1^+$). Mean + s.d. (n = 12 mice/group) from 3 pooled experiments. ***$P<0.0001$, by two-way analysis of variance (ANOVA), NS, not significant. (**e**) Representative photomicrographs and (**f**) quantitation of total GC area and SFliC-specific area in serial MLN sections from NI or sFliC prime–boosted *Irf8*$^{fl/fl}$(black) or *Cd11c-cre.Irf8*$^{fl/fl}$ (white) mice. (**e**) Scale bar = 200 µm. First row, GC identification (PNA, blue; IgD, brown). Second row, sFliC-specific GC (sFliC, blue; IgD, brown). (**f**) Mean + s.d. (n = 8 sections/group, from 2 experiments). Number of (**g**) GC B cells ($TCR^-CD138^-GL7^+CD95^+$) and (**h**) Tfh cells ($CXCR5^+PD1^+$) as assessed by fluorescence-activated cell sorting (FACS). Mean + s.d. (n = 8 mice/group) from 2 experiments. **$P<0.001$, by two-way ANOVA.

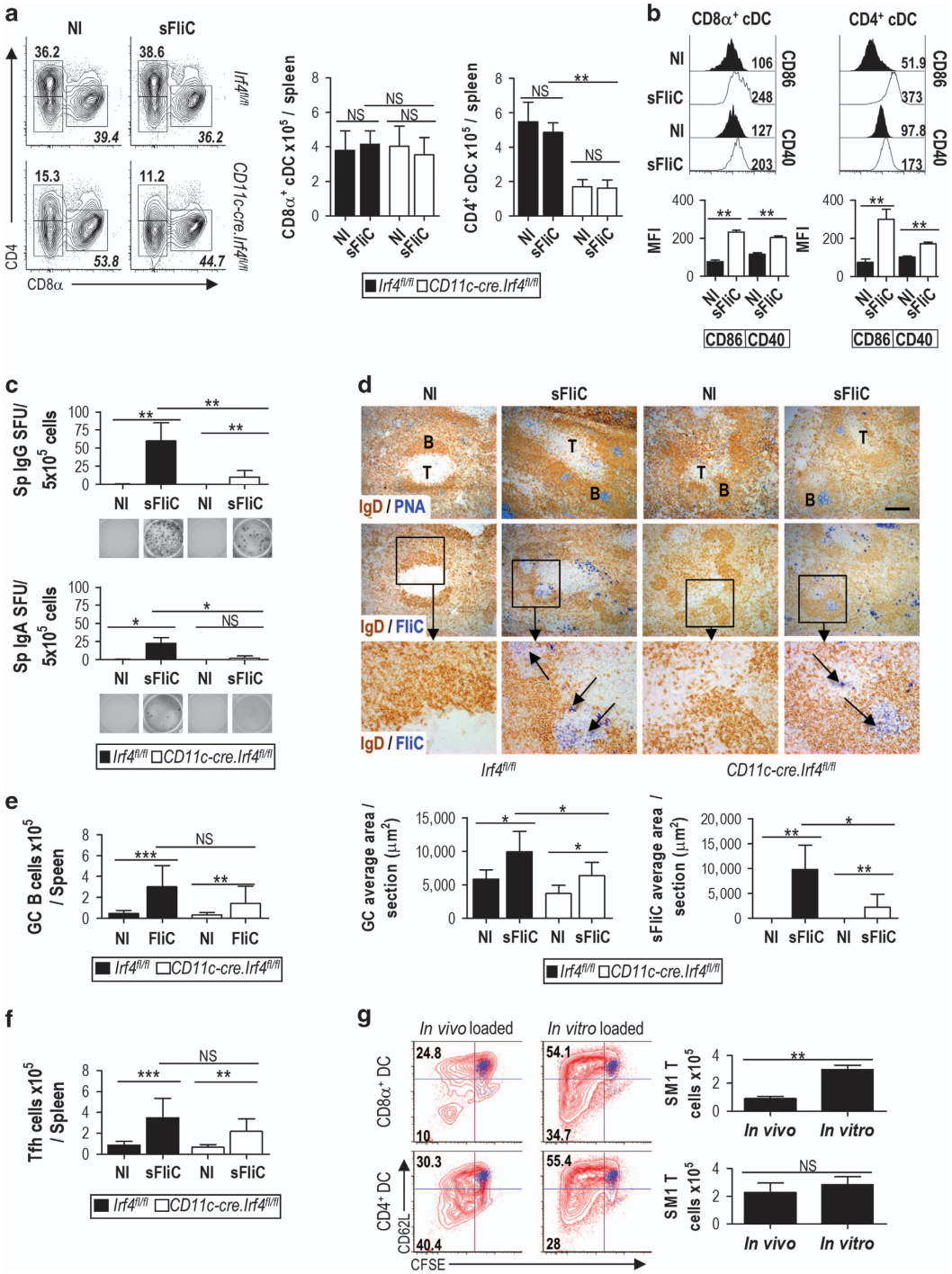

Figure 5 Systemic responses to soluble flagellin (sFliC) are reduced in the absence of splenic CD4$^+$CD11b$^+$ classical dendritic cells (cDCs). *Irf4*$^{fl/fl}$ (black) or *Cd11c-cre.Irf4*$^{fl/fl}$ (white) mice were either nonimmunized (N.I.) or sFliC prime–boosted. (**a**) Representative plots (with percentage) and absolute number (right graphs) of CD4$^+$ and CD8α$^+$ splenic cDCs. (**b**) Representative histograms and pooled mean fluorescence intensity (MFI) of CD86 and CD40 levels on CD4$^+$ and CD8α$^+$ splenic cDC subsets 24 h after sFliC immunization. Mean + s.d. ($n = 4$ mice/group) from 1 representative experiment of 3 performed. ***$P < 0.0001$, by two-way analysis of variance (ANOVA), NS, not significant. (**c**) ELISPOT (Enzyme-Linked ImmunoSpot) analysis of splenic sFliC-specific G (IgG) and immunoglobulin A (IgA) cells. Lower panels show representative pictures. Mean + s.d. ($n = 12$ mice/group) of 3 experiments. *$P < 0.01$, **$P < 0.001$, by two-way ANOVA. (**d**) Representative micrographs of (first row) GC (PNA, blue; IgD, brown), (second row), sFliC-specific GC (sFliC, blue; IgD, brown), and (last row), high magnification of identified area. Scale bar = 200 μm. Quantification of total GC area and sFliC-specific area per section. Mean + s.d. ($n = 10$ sections/group) of 2 experiments. Total number of (**e**) Splenic GC and (**f**) T follicular helper (Tfh) cells (CXCR5$^+$PD1$^+$) cells. Mean + s.d. ($n = 12$ mice/group) of 3 experiments. ***$P < 0.0001$, by two-way ANOVA. (**g**) CD4$^+$ and CD8α$^+$ splenic cDC subsets were cell sorted (97% purity) from wild-type (WT) mice 24 h after immunization with sFliC and cultured for 4 days with carboxyfluorescein succinimidyl ester (CFSE)-labeled SM1 transgenic T cells in a 1:30 ratio. cDCs were used a sorted (*in vivo* loaded) or additional 2 μg of sFliC was added to the culture (*in vitro* loaded). T-cell division was assessed by CFSE dilution and CD62L expression, and blue overlay represents culture of only T cells. Representative histograms from three independent experiments are shown. Data are shown as mean + s.d. ($n = 4$ mice/group) and are representative of two independent experiments polled together. **$P < 0.001$, by Mann–Whitney test.

cDCs could potentially contribute to antigen presentation. To address this possibility, WT mice were immunized with sFliC for 24 h and $CD4^+CD11b^+$ and $CD8\alpha^+CD11b^-$ splenic cDCs were FACS sorted and co-cultured with SM1 T cells. Both $CD4^+CD11b^+$ and $CD8\alpha^+CD11b^-$ cDCs induced SM1 T-cell proliferation, although $CD8\alpha^+CD11b^-$ cDC did so less efficiently (**Figure 5g**). The difference in T-cell proliferation after co-culture probably reflects differences in antigen capture *in vivo* rather than an intrinsic difference in their capacity to present antigen as T-cell proliferation was similar when sFliC was added to the cultures *ex vivo* (**Figure 5g**). Collectively, these results suggest that IRF4-dependent and -independent cDCs contribute to the splenic sFliC-specific response.

Mucosal DP cDCs contribute to sFliC-specific Ab responses in the BM

To study the persistence of the anti-sFliC Ab response, we next examined the BM, representing an important site for maintenance of long-lived plasma cells. Strikingly, although sFliC-specific IgG^+ and IgA^+ ASCs were readily detected in the BM of *Irf4*$^{fl/fl}$ mice, they were completely absent in the BM of *Cd11c-cre.Irf4*$^{fl/fl}$ mice (**Figure 6a**). In contrast, the BM of *Cd11c-cre.Irf8*$^{fl/fl}$mice had a similar number of sFliC-specific ASCs as control *Irf4*$^{fl/fl}$ mice (**Figure 6b**). The complete lack of sFliC-specific ASCs in the BM of *Cd11c-cre.Irf4*$^{fl/fl}$ mice suggested that mucosal DP cDCs may contribute to the long-term Ab response in the BM. To assess this possibility, expression of the intestinal-associated signature integrin $\alpha_4\beta_7$ (refs. [32,33]) was examined on BM sFliC-specific plasma cells from WT mice primed–boosted with sFliC. A sFliC-specific population of plasma cells was detected in the BM of sFliC immunized but not unimmunized mice, as assessed by flow cytometry (**Figure 6c**). Furthermore, a proportion of these sFliC-specific but not non-sFliC-specific BM plasma cells expressed $\alpha_4\beta_7$ (**Figure 6c**). Consistent with these findings, sFliC-specific cells expressing $\alpha_4\beta_7$ were detected on cytospins preparations of enriched $CD138^+$ BM cells from the same mice (**Figure 6d**). Finally, the data suggest that loss of DP cDCs should have an effect on the total serum antibody response to sFliC. IgG titers were >90% reduced in *Cd11c-cre.Irf4*$^{fl/fl}$ mice compared with control mice and IgA was undetectable (**Figure 6e**). Collectively, these results suggest that mucosal DP cDC priming of antibody responses in the MLN can enhance sFliC-specific ASC numbers in the BM following IP immunization with sFliC.

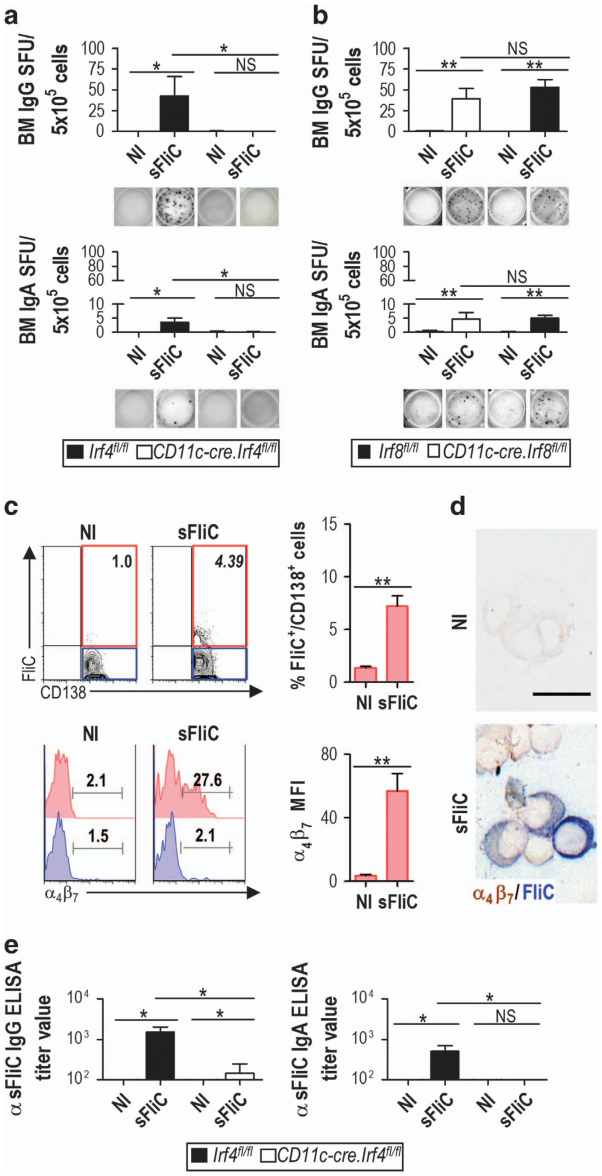

Figure 6 The mucosal response to soluble flagellin (sFliC) contributes to the systemic antibody response. *Irf4*$^{fl/fl}$(black) or *Cd11c-cre.Irf4*$^{fl/fl}$ (white) mice were either nonimmunized (NI) or sFliC prime–boosted. (**a**) ELISPOT (Enzyme-Linked ImmunoSpot) analysis of sFliC immunoglobulin G (IgG) and immunoglobulin A (IgA) responses in the bone marrow (BM). Number of spot-forming units (SFUs) per 5×10^5 cells (graphs) and representative pictures of wells (lower panels). Data are shown as mean + s.d. ($n = 12$ mice/group) of three independent experiments pooled together. *$P < 0.01$, **$P < 0.001$, by two-way analysis of variance (ANOVA). (**b**) *Cd11c-cre.Irf8*$^{fl/fl}$ (white) or *Irf8*$^{fl/fl}$control mice (black) were either NI or sFliC primed–boosted. ELISPOT analysis of sFliC IgG and IgA responses in the BM. Data are shown as mean + s.d. ($n = 8$ mice/group) of two independent experiments pooled together. *$P < 0.01$, by two-way ANOVA. (**c**) Wild-type (WT) mice were NI or sFliC primed–boosted. BM $CD138^+$ cells were intracellularly stained with sFliC-biotinylated, expression of $\alpha_4\beta_7$ is shown in $sFliC^+$ and $sFliC^-$ $CD138^+$ cells by fluorescence-activated cell sorting (FACS) and (**d**) cytospins show $\alpha_4\beta_7$ (brown) and sFliC (blue) in pre-enriched $CD138^+$ cells. Scale bar = 20 μm. Representative plots and photomicrographs ($n = 4$ mice/group) from 2 independent experiments. (**e**) Serum anti-sFliC IgG and IgA evaluated by enzyme-linked immunosorbent assay (ELISA). Data are shown as mean + s.d. ($n = 12$ mice/group) and are representative of three independent experiments pooled together. *$P < 0.01$, by two-way ANOVA.

DISCUSSION

Previously, it has been shown that systemic immunization with sFliC induces parallel Ab responses in systemic and mucosal secondary lymphoid tissues, with the latter responses associated with a rapid TLR5-dependent accumulation of antigen-carrying $CD103^+$ cDCs in the intestinal-draining MLN.[15] Here we demonstrate that mucosal DP cDCs are required for the anti-sFliC response in the MLN and provide evidence that plasma cells derived from this response can ultimately take up residence in the BM and contribute to the systemic antibody

pool. The ability of sFliC to efficiently engage the mucosal immune system after a systemic immunization may confer a significant advantage to sFLiC-containing vaccines, such as the influenza–flagellin fusion vaccine that has shown safety and potential not only in healthy adults but also in the elderly[9,10] who often induce poor Ab responses.[34]

Although multiple MLN cDC subsets can induce T-cell responses to sFliC after antigen loading *in vitro*,[35] we demonstrate here that only DP cDCs drive T- and B-cell responses in the MLN *in vivo*. The reasons why IRF4-dependent DP cDCs are so critical in driving sFliC-specific T-cell responses in the MLN remain to be fully elucidated but are likely multifactorial. Previous studies have demonstrated that IRF4-dependent cDCs have an enhanced intrinsic capacity to prime $CD4^+$ T cells compared with IRF8-dependent cDCs.[23,36] Interestingly, sFliC induced MyD88-dependent accumulation was similar after secondary immunization, even in the presence of high-affinity sFliC Ab,[2,3] indicating a high efficiency of sFliC capture by TLR5. These results are consistent with prior observations that small amounts of sFliC are required for its immune modulatory effects[37] and further suggest that inclusion of sFliC in boost as well as in prime vaccines could further promote mucosal immune system engagement. Notably, recognition of intestinal microbiota-derived flagellin is also TLR5 dependent and boosts vaccine responses through the action of clodronate-sensitive (presumably monocyte derived) cells.[38] Given our current findings, the cross-talk between these cells and DP cDCs in driving the microbiota-derived flagellin response warrants further study. sFliC-specific responses in the spleen were reduced in *Cd11c-cre.Irf4*$^{fl/fl}$ mice. Splenic $CD4^+$ cDCs from immunized WT mice efficiently primed sFliC-specific T cells *ex vivo* and these cells were selective reduced in *Cd11c-cre.Irf4*$^{fl/fl}$ mice, collectively indicating that IRF4-dependent $CD4^+$ cDCs are required for optimal sFliC-specific responses in the spleen. Despite these findings, sFliC-induced Tfh cell accumulation was not significantly altered, and sFliC-specific GCs were readily detectable in the spleen in the absence of IRF4-dependent cDCs, suggesting that additional antigen-presenting cells contribute to the sFliC-specific response at this site. Although the identity of these IRF4-independent antigen-presenting cells remains to be identified, splenic $CD8^+$ cDCs isolated from immunized mice induced limited sFliC-specific T-cell generation *ex vivo*, indicating that IRF8-dependent cDCs may contribute to this response. Collectively, these findings indicate that the cellular and molecular mechanisms driving sFliC-specific immune responses in the spleen and MLN are, in part, distinct.

These findings are consistent with prior studies demonstrating that immune responses induced by sFliC are both complex and site specific. Thus, although sFliC drives both an IgG and IgA response in the MLN, it drives primarily an IgG response in the spleen.[15] sFliC-specific IgA responses are TLR5 dependent,[15] whereas sFliC-specific IgG responses, in particular IgG1 responses, can occur through TLR5- and inflammasome-independent pathways.[13,39] Furthermore, sFliC-specific T-cell responses in the spleen are also less dependent on TLR5 than in the MLN[15] and splenic cDCs have been reported to express lower levels of TLR5 in comparison with cDCs from the intestinal mucosa.[40] Thus, the features of sFliC that enable it to have these effects are likely to relate to it being the ligand for TLR5 and its modest molecular size. The accumulation of $CD103^+$ cDCs in the MLN after sFliC immunization is TLR5 dependent[41] and SI-LP cDCs with a similar phenotype as DP cDC ($CD103^+CD11c^{hi}CD11b^{hi}$) have been shown to express high levels of TLR5.[42] In contrast, splenic cDCs do not appear to express as high levels of TLR5 as SI-LP cDCs.[40] Indeed, consistent with the need for TLR5 expression, we show that MyD88 expression in DP cDCs is needed for their accumulation in the MLN after immunization. Furthermore, TLR5 itself can enhance presentation of antigen through MyD88-independent mechanisms, indicating its function in promoting antigen presentation may be multifactorial.[13] Although these points may help explain why DP cDCs have an enhanced capacity to capture and present sFliC, it does not explain how sFliC gets to this site. This could relate to the use of highly purified, monomeric flagellin in these studies. sFliC has a relatively modest size of $\sim$50 kDa, meaning it can disseminate readily through the host after systemic immunization. Other studies have found molecules of a similar or greater size are also able to disperse rapidly throughout the host and prime responses in multiple sites.[43] While not addressed in the present study, it remains possible that DP cDC promote sFliC responses in part through direct interactions with B cells. A more detailed understanding of the molecular pathways by which antigen-presenting cell subsets orchestrate these diverse responses to sFliC should provide important information regarding sFliC usage in future vaccines.

Interestingly, IgA^+ and IgG^+ sFliC-specific ASCs were completely absent in the BM of sFliC immunized *Cd11c-cre.Irf4*$^{fl/fl}$ mice and we found that a proportion of sFliC-specific ASCs accumulating in the BM of sFliC immunized WT mice expressed the intestinal homing receptor $\alpha_4\beta_7$. This suggests that some of these ASCs were initially generated in intestinal lymph nodes.[44] Nevertheless, this does not necessarily mean all ASCs in the BM derive from the mucosa, nor does it exclude the possibility that long-lived ASCs can be generated in other sites, as we detected sFliC-specific ASCs in the spleen. For instance, it has been shown that long-lived plasma cells can be found in the spleen, as well as the BM, indicating multiple reservoirs can exist.[45] Collectively, these results suggest that the priming of responses in the MLN by DP cDCs may contribute to the accumulation of sFliC-specific plasma cells in the BM and hence to sFliC-specific serological memory. In support of this, sFliC-specific IgA^+ plasma cells are detected in the MLN and not the spleen during a primary response[15] and long-lived BM plasma cell responses can be induced in splenectomized mice after immunizing mice orally with high doses of ovalbumin and cholera toxin.[46] The ability of sFliC to engage DP cDCs, and in so doing promote both mucosal and serological antibody responses, could mean that optimal serological memory requires engagement of the mucosa. Alternatively, this effect

could be restricted to the response to sFliC, or just last for the period assessed in this study. Indeed, the ablated ASC response in the MLN and SI-LP observed when mucosal DP cDCs were reduced was not observed in the spleen, indicating that other pathways for the generation of ASCs remain. Thus, this reduction in ASC in the BM may not be permanent or absolute. Either way, it suggests it may be possible to use flagellin to direct mucosally induced plasma cells to the BM. Understanding this may help identify how to enhance the longevity of responses to vaccines that can be dramatically different depending upon their nature and how they are administered.[47]

In summary, our results show how sFliC, by targeting DP cDCs, can overcome the difficulties in inducing a mucosal response after systemic immunization. This highlights the interplay between the mucosal and systemic immune systems and offers an alternative and highly desirable approach to drive long-lived systemic immunity by engaging mucosal DP cDCs.

METHODS

Mice. *Cd11c-cre.MyD88*$^{fl/fl}$,[28] *Cd11c-cre.Irf4*$^{fl/f}$,[21] and *Cd11c-creIrf8*$^{fl/fl}$ mice[26] were maintained at the Biomedical Center at Lund University (Lund, Sweden). SM1 transgenic[29] mice were maintained at the University of Birmingham Biomedical Service Unit (Birmingham, UK). Specific pathogen-free 6–8-week-old C57BL/6 mice were purchased from Harlan Sprague-Dawley (Huntington, UK). Littermates or age-matched mice were used for all experiments where appropriate. All animal procedures were carried out in strict accordance with the Lund/Malmö Animal Ethics Committee, the University of Birmingham Ethics Committee, and the UK Home Office approval (project license 30/2850).

Antigen preparation and immunizations. sFliC was generated as previously described.[3] Briefly, the FliC gene from *Salmonella* Typhimurium was cloned into pETT22b$^+$ via *nde*I and *xho*I sites to incorporate a poly-histidine tag. After induction, His-tagged recombinant protein was enriched by nickel affinity chromatography resulting in a purity of 95%. Following dialysis, the protein was further purified by immunoprecipitation with a sFliC-specific monoclonal. Each batch was tested by immunization of WT and TLR5-deficient mice. Batches were only accepted if cDCs in the spleen and MLN matured in WT but not TLR5-deficient mice. Mice were immunized IP with 20 μg recombinant sFliC, IP boosted 21 days later with the same dose, and responses were assessed 4 days after boost.

Cell isolation and flow cytometry. Single-cell suspensions from spleen and MLN and BM were generated by mechanical disruption. When evaluating cDCs, MLN and spleen were enzymatic digested with collagenase IV digestion (400 U ml^{-1}; 25 min; 37 °C). Cell suspensions from SI-LP were generated as previously described[48] using Liberase (0.2–0.3 WunchU ml^{-1}, Roche, Basel, Switzerland). Cells were processed for flow cytometry according to standard procedures.[15] Data acquisition was performed on a LSRII (BD Bioscience, San Jose, CA) or a CyAn ADP (Beckman Coulter, Brea, CA) and analyzed using FlowJo software 9.8.2. (Tree Star, Aghland, OR). All antibodies used are listed in **Supplementary Table S1**.

Mixed BM chimeras. BM chimeras were generated by transferring BM cells (1.5×10^6 cells) intravenously from the indicated donor mice into lethally irradiated (900 rad) recipient mice. Mixed BM chimeras were generated by transferring a 50:50 mix of BM from the indicated strains. Mice were used for immunization experiments 8 weeks after BM transfer.

In vitro* co-culture to evaluate cDC antigen loading *in vivo. Spleen and MLN were collected 24 h post IP immunization with sFliC (20 μg), and single-cell suspensions prepared as described above. The cDCs were pre-enriched using MACS beads (anti-CD19, CD5 and DX5). Cell suspensions were subsequently stained with anti-CD11c, MHC-II, CD103, and CD11b (MLN) or CD11c, MHCII, CD4, and CD8 (spleen) and the indicated cDC subsets FACS sorted on a BD FACSAria Fusion. The following subsets were isolated: SP (CD103$^+$CD11b$^-$) and DP (CD103$^+$CD11b$^+$) cDCs from the MLN from the CD11c^{hi}MHC-II$^+$ population. From the spleen using again a pregate CD11c^{hi}MHC-II$^+$ CD8α$^+$CD11b$^-$ and CD4$^+$CD11b$^+$ cDCs were sorted to a purity of at least 97%. SM1 T cells were MACS enriched (CD5$^+$ selection) and carboxyfluorescein succinimidyl ester labeled. The cDCs and T cells were co-cultured for 4 days (1:30 ratio cDC/T) before flow cytometry analysis.

ELISPOT analysis. ELISPOT was performed as described previously.[15] In brief, 5×10^5 cells were added per well in triplicates in a sFliC precoated plate and cultured for 6 h at 37 °C. After incubation, plates were incubated overnight at 4 °C with alkaline phosphate-conjugated anti-IgG and IgA (Southern Biotech, Birmingham, AL). Reaction was developed with SIGMA Fast BCIP/NBT (Sigma Aldrich, St. Louise, MO). Spots were counted using the AID ELISPOT Reader System and AID software version 3.5 (Autoimmune Diagnostika, Strassberg, Germany). Counts were expressed as spot-forming units per 5×10^5 cells.

Immunohistochemistry and confocal microscopy. Immunohistology was performed as described previously.[3] Cryosections were incubated with primary unconjugated Abs for 45 min at room temperature before addition of either horseradish peroxidase-conjugated or biotin-conjugated secondary antibodies. sFliC-binding cells were identified as previously described[3,15] using biotinylated sFliC. When using cytospins, 1×10^5 cells were used per cytospin and cells were fixed in cold acetone for 10 min. Signal was detected using diaminobenzidine for horseradish peroxidase activity and naphthol AS-MX phosphate with Fast Blue salt and levamisole for alkaline phosphatase activity. Images were acquired using a Leica (Milton Keynes, UK) microscope DM6000 using 10 × and 20 × objectives or the Zeiss (Jena, Germany) Axio ScanZ1 Slide Scanner using 10 × objective. Quantification of GC area was performed using Zen 2012 (blue edition, Jena, Germany) software.

Confocal was performed on frozen sections as previously described.[49] Staining was performed in phosphate-buffered saline containing 10% fetal calf serum, 0.1% sodium azide, and sections were mounted in 2.5% 1,4-Diazabicyclo(2,2,2)octane (pH 8.6) in 90% glycerol in phosphate-buffered saline. Confocal images were acquired using a Zeiss LSM510 laser scanning confocal microscope with a Zeiss AxioVert 100M. Signals obtained from lasers were scanned separately and stored in four non-overlapping channels as pixel digital arrays of 2,048 × 2,048 (10 × objective) or 1,024 × 1,024 (63 × objective).

FliC-specific enzyme-linked immunosorbent assay. Enzyme-linked immunosorbent assay plates were coated with 5 μg ml^{-1} of sFliC (2 h at 4 °C) and blocked with 1% bovine serum albumin overnight at 4 °C. Serum, diluted 1:100 in phosphate-buffered saline–0.05% Tween, was added and diluted stepwise. To measure total Ab titers serum was diluted in 1:1,000 and added and further diluted stepwise on uncoated plates. Following incubation for 1 h at 37 °C, plate-bound antibodies were detected using alkaline phosphatase-conjugated goat anti-mouse IgG, IgG1, and IgA (Southern Biotech). Reaction was developed with Sigma-Fast *p*-nitrophenylphosphate (Sigma Aldrich). Relative reciprocal titers were calculated by measuring the dilution at which the serum reached a defined OD^{405}.

Statistics. Statistics were calculated using the nonparametric Mann–Whitney sum of ranks test or two-way analysis of variance as appropriate using the GraphPad Prism software (GraphPad, La Jolla, CA).

SUPPLEMENTARY MATERIAL is linked to the online version of the paper at http://www.nature.com/mi

ACKNOWLEDGMENTS

This work was supported by grants from the BBSRC UK to A.F.C., U21 staff fellowship program and Wellcome Trust ISSF Mobility grant to A.F.-L., and grants from the Danish Council for Independent Research (Sapere Aude III) and the Swedish Medical Research Council to W.W.A. We thank B.N. Lambrecht for original provision of *Irf8*$^{fl/fl}$mice. We are grateful to K. Kotarsky and A. Selberg for animal typing and husbandry (Lund University), Matthew Graeme MacKenzie for cell sorting, and Ian Ricketts at the Biomedical Service Unit at the University of Birmingham.

AUTHOR CONTRIBUTIONS

Conceptualization: A.F.-L., A.F.C. and W.W.A. Methodology: M.W.D., K.H., B.J.L. and B.J.L. Investigation: A.F.-L., K.M.L., E.K.P., S.B., and J.L.M. Resources: C.N.C. and D.R.W. Writing, original draft: A.F.-L., A.F.C., B.J.L. and W.W.A. Writing, review and editing: A.F.-L., A.F.C., I.R.H., B.J.L. and W.W.A. Funding acquisition: A.F.-L., A.F.C., and W.W.A.

DISCLOSURE

The authors declared no conflict of interest.

REFERENCES

1. Hayashi, F. *et al.* The innate immune response to bacterial flagellin is mediated by Toll-like receptor 5. *Nature* **410**, 1099–1103 (2001).
2. Bobat, S. *et al.* Soluble flagellin, FliC, induces an Ag-specific Th2 response, yet promotes T-bet-regulated Th1 clearance of Salmonella typhimurium infection. *Eur. J. Immunol.* **41**, 1606–1618 (2011).
3. Cunningham, A.F. *et al.* Responses to the soluble flagellar protein FliC are Th2, while those to FliC on Salmonella are Th1. *Eur. J. Immunol.* **34**, 2986–2995 (2004).
4. Didierlaurent, A. *et al.* Flagellin promotes myeloid differentiation factor 88-dependent development of Th2-type response. *J. Immunol.* **172**, 6922–6930 (2004).
5. McSorley, S.J., Ehst, B.D., Yu, Y. & Gewirtz, A.T. Bacterial flagellin is an effective adjuvant for CD4+ T cells in vivo. *J. Immunol.* **169**, 3914–3919 (2002).
6. Kajikawa, A. *et al.* Construction and immunological evaluation of dual cell surface display of HIV-1 gag and Salmonella enterica serovar Typhimurium FliC in Lactobacillus acidophilus for vaccine delivery. *Clin. Vaccine Immunol.* **19**, 1374–1381 (2012).
7. Liu, G. *et al.* Immunogenicity and efficacy of flagellin-fused vaccine candidates targeting 2009 pandemic H1N1 influenza in mice. *PLoS One* **6**, e20928 (2011).
8. Sun, Y. *et al.* Flagellin-PAc fusion protein is a high-efficacy anti-caries mucosal vaccine. *J. Dent. Res.* **91**, 941–947 (2012).
9. Taylor, D.N. *et al.* Induction of a potent immune response in the elderly using the TLR-5 agonist, flagellin, with a recombinant hemagglutinin influenza-flagellin fusion vaccine (VAX125, STF2.HA1 SI). *Vaccine* **29**, 4897–4902 (2011).
10. Turley, C.B. *et al.* Safety and immunogenicity of a recombinant M2e-flagellin influenza vaccine (STF2.4xM2e) in healthy adults. *Vaccine* **29**, 5145–5152 (2011).
11. Zhang, B. *et al.* Viral infection. Prevention and cure of rotavirus infection via TLR5/NLRC4-mediated production of IL-22 and IL-18. *Science* **346**, 861–865 (2014).
12. Burdelya, L.G. *et al.* An agonist of toll-like receptor 5 has radioprotective activity in mouse and primate models. *Science* **320**, 226–230 (2008).
13. Letran, S.E., Lee, S.J., Atif, S.M., Uematsu, S., Akira, S. & McSorley, S.J. TLR5 functions as an endocytic receptor to enhance flagellin-specific adaptive immunity. *Eur. J. Immunol.* **41**, 29–38 (2011).
14. Flores-Langarica, A. *et al.* Soluble flagellin coimmunization attenuates Th1 priming to Salmonella and clearance by modulating dendritic cell activation and cytokine production. *Eur J Immunol* **45**, 2299–2311 (2015).
15. Flores-Langarica, A. *et al.* Systemic flagellin immunization stimulates mucosal CD103+ dendritic cells and drives Foxp3+ regulatory T cell and IgA responses in the mesenteric lymph node. *J. Immunol.* **189**, 5745–5754 (2012).
16. Bekiaris, V., Persson, E.K. & Agace, W.W. Intestinal dendritic cells in the regulation of mucosal immunity. *Immunol. Rev.* **260**, 86–101 (2014).
17. Joeris, T., Muller-Luda, K., Agace, W.W. & Mowat, A.M. Diversity and functions of intestinal mononuclear phagocytes. *Mucosal Immunol.* **10**, 845–864 (2017).
18. Edelson, B.T. *et al.* Peripheral CD103+ dendritic cells form a unified subset developmentally related to CD8alpha+ conventional dendritic cells. *J. Exp. Med.* **207**, 823–836 (2010).
19. Ginhoux, F. *et al.* The origin and development of nonlymphoid tissue CD103+ DCs. *J. Exp. Med.* **206**, 3115–3130 (2009).
20. Welty, N.E., Staley, C., Ghilardi, N., Sadowsky, M.J., Igyarto, B.Z. & Kaplan, D.H. Intestinal lamina propria dendritic cells maintain T cell homeostasis but do not affect commensalism. *J. Exp. Med.* **210**, 2011–2024 (2013).
21. Persson, E.K. *et al.* IRF4 transcription-factor-dependent CD103(+) CD11b(+) dendritic cells drive mucosal T helper 17 cell differentiation. *Immunity* **38**, 958–969 (2013).
22. Satpathy, A.T. *et al.* Notch2-dependent classical dendritic cells orchestrate intestinal immunity to attaching-and-effacing bacterial pathogens. *Nat. Immunol.* **14**, 937–948 (2013).
23. Schlitzer, A. *et al.* IRF4 transcription factor-dependent CD11b+ dendritic cells in human and mouse control mucosal IL-17 cytokine responses. *Immunity* **38**, 970–983 (2013).
24. Mayer, J.U., Demiri, M., Agace, W.W., MacDonald, A., Svensson-Frej, M. & Milling, S.W. Distinct subsets of IRF4+ dendritic cells drive Th2 responses in the small intestine and colon. *Nat. Commun* **31**, 44–50 (2017).
25. Gutweiler, S. *et al.* IRF4-dependent CD103+CD11b+ DCs and microbial signals critically regulate peristalsis and its cessation after intestinal surgery. *Gut* **66**, 2110–2120 (2017).
26. Luda, K.M. *et al.* IRF8 transcription-factor-dependent classical dendritic cells are essential for intestinal T cell homeostasis. *Immunity* **44**, 860–874 (2016).
27. Ohta, T. *et al.* Crucial roles of XCR1-expressing dendritic cells and the XCR1-XCL1 chemokine axis in intestinal immune homeostasis. *Sci. Rep.* **6**, 23505 (2016).
28. Hagerbrand, K., Westlund, J., Yrlid, U., Agace, W. & Johansson-Lindbom, B. MyD88 signaling regulates steady-state migration of intestinal CD103+ dendritic cells independently of TNF-alpha and the gut microbiota. *J. Immunol.* **195**, 2888–2899 (2015).
29. McSorley, S.J., Asch, S., Costalonga, M., Reinhardt, R.L. & Jenkins, M.K. Tracking salmonella-specific CD4 T cells in vivo reveals a local mucosal response to a disseminated infection. *Immunity* **16**, 365–377 (2002).
30. McSorley, S.J., Cookson, B.T. & Jenkins, M.K. Characterization of CD4+ T cell responses during natural infection with Salmonella typhimurium. *J. Immunol.* **164**, 986–993 (2000).
31. Willis, S.N. *et al.* Transcription factor IRF4 regulates germinal center cell formation through a B cell-intrinsic mechanism. *J. Immunol.* **192**, 3200–3206 (2014).
32. Mei, H.E. *et al.* Blood-borne human plasma cells in steady state are derived from mucosal immune responses. *Blood* **113**, 2461–2469 (2009).
33. Rott, L.S., Briskin, M.J. & Butcher, E.C. Expression of alpha4beta7 and E-selectin ligand by circulating memory B cells: implications for targeted trafficking to mucosal and systemic sites. *J. Leukoc. Biol.* **68**, 807–814 (2000).
34. Pinti, M. *et al.* Aging of the immune system: focus on inflammation and vaccination. *Eur. J. Immunol.* **46**, 2286–2301 (2016).
35. Atif, S.M., Uematsu, S., Akira, S. & McSorley, S.J. CD103-CD11b+ dendritic cells regulate the sensitivity of CD4 T-cell responses to bacterial flagellin. *Mucosal Immunol.* **7**, 68–77 (2014).
36. Vander Lugt, B. *et al.* Transcriptional programming of dendritic cells for enhanced MHC class II antigen presentation. *Nat. Immunol.* **15**, 161–167 (2014).
37. Lu, Y. & Swartz, J.R. Functional properties of flagellin as a stimulator of innate immunity. *Sci. Rep.* **6**, 18379 (2016).
38. Oh, J.Z. *et al.* TLR5-mediated sensing of gut microbiota is necessary for antibody responses to seasonal influenza vaccination. *Immunity* **41**, 478–492 (2014).

39. Lopez-Yglesias, A.H. *et al.* Flagellin induces antibody responses through a TLR5- and inflammasome-independent pathway. *J. Immunol.* **192**, 1587–1596 (2014).
40. Feng, T., Cong, Y., Alexander, K. & Elson, C.O. Regulation of Toll-like receptor 5 gene expression and function on mucosal dendritic cells. *PLoS ONE* **7**, e35918 (2012).
41. Flores-Langarica, A. *et al.* Systemic flagellin immunization stimulates mucosal CD103 + dendritic cells and drives Foxp3 + regulatory T cell and IgA responses in the mesenteric lymph node. *J. Immunol.* **189**, 5745–5754 (2012).
42. Fujimoto, K. *et al.* A new subset of CD103 + CD8alpha + dendritic cells in the small intestine expresses TLR3, TLR7, and TLR9 and induces Th1 response and CTL activity. *J. Immunol.* **186**, 6287–6295 (2011).
43. Bonifaz, L.C. *et al.* In vivo targeting of antigens to maturing dendritic cells via the DEC-205 receptor improves T cell vaccination. *J. Exp. Med.* **199**, 815–824 (2004).
44. Mora, J.R. & von Andrian, U.H. Differentiation and homing of IgA-secreting cells. *Mucosal Immunol* **1**, 96–109 (2008).
45. Sze, D.M., Toellner, K.M., Garcia de Vinuesa, C., Taylor, D.R. & MacLennan, I.C Intrinsic constraint on plasmablast growth and extrinsic limits of plasma cell survival. *J. Exp. Med.* **192**, 813–821 (2000).
46. Lemke, A., Kraft, M., Roth, K., Riedel, R., Lammerding, D. & Hauser, A.E. Long-lived plasma cells are generated in mucosal immune responses and contribute to the bone marrow plasma cell pool in mice. *Mucosal Immunol.* **9**, 83–97 (2016).
47. Slifka, M.K., Antia, R., Whitmire, J.K. & Ahmed, R. Humoral immunity due to long-lived plasma cells. *Immunity* **8**, 363–372 (1998).
48. Jaensson, E. *et al.* Small intestinal CD103 + dendritic cells display unique functional properties that are conserved between mice and humans. *J. Exp. Med.* **205**, 2139–2149 (2008).
49. Mohr, E. *et al.* Dendritic cells and monocyte/macrophages that create the IL-6/APRIL-rich lymph node microenvironments where plasmablasts mature. *J. Immunol.* **182**, 2113–2123 (2009).